Rotational symmetry breaking of nuclear motion in the Jahn-Teller X_3 molecule due to Casimir-Polder interaction

A. D. Lyakhov [1], A. S. Ovchinnikov [1,2], I. G. Bostrem,[1] and J. Kishine [3,4]

[1] *Institute of Natural Science and Mathematics, Ural Federal University, Ekaterinburg 620002, Russia*

[2] *Institute of Metal Physics, Ural Division, Russian Academy of Sciences, Ekaterinburg 620219, Russia*

[3] *Division of Natural and Environmental Sciences, The Open University of Japan, Chiba 261-8586, Japan*

[4] *Quantum Research Center for Chirality, Institute for Molecular Science, Okazaki 444-8585, Japan*

(Received 4 June 2023; revised 6 September 2023; accepted 11 September 2023; published 20 September 2023)

The Casimir-Polder interaction between the Jahn-Teller X_3 molecule with the linear $E \otimes e$ problem and a gyrotropic medium is considered. Due to the interaction, the molecule plane is reoriented perpendicularly to the interface surface to lift degeneracy of circular motion of molecule nuclei. A direct consequence of the broken rotational symmetry is the appearance of the orbital magnetic moment and accumulation of the topological Berry phase.

DOI: 10.1103/PhysRevB.108.115429

I. INTRODUCTION

The Casimir-Polder effect is a well-known phenomenon in physics that describes an attraction between a neutral atom and a surface due to quantum fluctuations [1,2]. Recently, it has been shown that the existence of degeneracy of low-lying atomic energy levels plays an important role in this effect and may results in the appearance of the Casimir torque acting on the atom [3]. At the same time, the dynamical Jahn-Teller (JT) effect, which is manifested as instability of molecular configurations in electronically degenerate states, has a long history of investigations as well [4]. However, these two areas of research have remained largely separate, despite the potential for cross-disciplinary insights.

The primary goal of this paper is to bridge the gap between these two fields by exploring the rotational symmetry breaking mechanism suggested by Silveirinha [3]. The use of JT molecules appears to be an appropriate way to verify this proposition. Specifically, we suggest using the Jahn-Teller X_3 molecules, belonging to the point group symmetry C_{3v}, which presents the well-known linear $E \otimes e$ problem [5]. When the molecule is brought close to a surface of the gyrotropic media, it experiences attraction to the surface due to the Casimir-Polder force. Special features of the rotovibrational spectrum of the JT molecule and broken time-reversal symmetry in the gyrotropic medium make it possible to realize in practice the model of rotational symmetry breaking in a Kramers two-level system. According to this analysis, two Kramers pairs of ground and excited states of an atom are coupled together by electric dipole transitions in such a way that atomic electric polarizability may be generically nonreciprocal. Being placed nearby a nonreciprocal substrate the atom is subjected to Casimir torque, which may reorient the atom plane of polarization. As a result, the ground-state Kramers degeneracy is lifted and the new stable state has a broken rotational (time-reversal) symmetry, which leads to the appearance of a nonzero orbital magnetic dipole moment.

Note that the above scenario becomes relevant only for dipolar-unstable polyatomic systems, i.e., for systems for which the JT-active symmetrized displacements of e type produce a dipole moment. In this regard, breaking of the high-symmetry configuration in the simplest linear molecules, triatomics, may be described by two bending normal displacements Q_x and Q_y, which form a twofold degenerate pair. However, there is no JT effect in their twofold degenerate states Π, Δ, Φ, ..., nor is there symmetry breaking induced by the Renner-Teller effect in these states [6,7]. The only source of symmetry-breaking bending in linear molecules is the pseudo-JT effect [8,9], but this case requires separate consideration. It remains, therefore, that suitable objects for implementation of the mechanism can be either trigonal molecular systems X_3 or square-planar molecular systems ML_4 (see Table 2.2 in Ref. [4]). In the first case, the alkali trimers Li_3, Na_3, and K_3 could be good candidates. These molecules are stable and possess an electronic ground-state E term in the regular triangular configuration [10]. In addition, the choice is of interest, because guiding of ultracold alkali monoatoms has been exploited in surface-mounted structures (atom chips) [11,12].

To make quantitative estimates from our treatment that might be observed, we use data on Li_3, which has been the subject of many previous studies [13–15]. The floppy cluster Li_3 forms the D_{3h} equilateral triangle, which undergoes a JT distortion to C_{2v} symmetry [16]. The distortion produces three equivalent potential energy minima separated by small barriers so that the molecule becomes fluxional due to pseudorotation between the different minima. This effect was first verified in ESR measurements of $^{18}Li_3$ and $^{21}Li_3$ trapped in cold argon matrices [17].

Given the rotovibrational spectrum of the JT $E \otimes e$ problem, we found that the dynamic polarizability, $\hat{\alpha}(\omega)$, is described by a second-rank tensor with nonzero antisymmetric part. This calculation is based on the assumption that at low temperatures, polarizability of the X_3 molecule in the

ground degenerate E state is limited only to transitions between the lowest rotational states, which occur due to nuclear displacements. Next, a vacuum fluctuation-induced Casimir-Polder energy of a coupling between the JT X_3 molecule and a surface of the gyrotropic medium is defined with the aid of the calculated $\hat{\alpha}(\omega)$. This interaction energy turns out to be attractive. At this point, it should be briefly mentioned that there were studies in which the Casimir-Polder interaction between a chiral molecule and a surface of the chiral medium was treated in detail [18,19]. It was shown that this interaction can be either attractive or repulsive, depending on the chirality of the molecule and the medium. This chirality-selective behavior could be a valuable tool for enantiomer separation. In our case of nonchiral molecules, however, even more important is the fact that the Casimir-Polder energy depends on an orientation of the molecule plane relative to the interface surface. A possible consequence of this interaction is the emergence not only of a Casimir force but also of a Casimir torque [20]. A similar situation arises in Casimir interaction of two birefringent plates [21,22], corrugated metallic plates [23], and topological Weyl semimetals [24]. In particular, we note Ref. [25], where reorientation of a carbon dioxide CO_2 linear molecule close to graphene membranes was analyzed.

Apart from the molecule dynamical polarizability, a calculation of the Casimir-Polder energy requires knowledge of the scattered dyadic (tensor) Green function of the surrounding electromagnetic field. Here we use the formalism developed in Refs. [3,26], in which the gyrotropic half-space is modeled by magnetized plasma and the scattered dyadic Green function is determined by electromagnetic waves on the surface of the material in the presence of an external in-plane magnetic field. It should be emphasized that the main function of the magnetic field is to break time-reversal symmetry inside the medium that results in a broken rotational symmetry of nuclear motion in the JT X_3 molecule by means of Casimir-Polder coupling.

When time-reversal symmetry is broken, the Kramers degeneracy of the ground state is lifted that gives rise to a nonzero orbital magnetic moment due to directed rotation of the molecule nuclei. An interesting feature of the induced orbital magnetic moment is that it depends entirely upon parameters of nuclear vibrations and the magnetic field inside the gyrotropic substrate is only a trigger for its appearance. However, this magnetic moment lies strictly in a direction opposed to the field.

Remarkably, the Kramers degeneracy lifting produces a nonzero Berry phase that has been pointed out in Ref. [27] for JT molecules, though without specifying a way of the degeneracy lifting. Thus, the Berry phase is tied with the persistent nuclear current in a similar manner as breaking of time-reversal symmetry in topological isolators or photonic topological insulators causes a nonzero accumulation of the Berry phase over the whole Brillouin zone (Chern number) and results in the topologically protected transport edge modes [28,29].

The remainder of this paper is organized as follows. In Sec. II, the rotovibrational spectrum of the classical JT $E \otimes e$ problem is introduced. The calculation of dynamical polarizability based on this spectrum is carried out in Sec. III. The derivation of the scattered dyadic Green function of the electromagnetic field is given in Sec. IV. Here, the energy of the Casimir-Polder interaction is discussed for two possible orientations of the X_3 molecule relative to the interface plane. The orbital magnetic moment and the Berry phase associated with nuclei motion are found in Sec. V. The paper is summarized and concluded in Sec. VI.

II. JT SPECTRUM

The $E \otimes e$ problem is one of the simplest and most common JT problems, when a polyatomic molecular system in a twofold orbitally degenerate E state interacts with doubly degenerate vibrational e modes. This JT problem with linear terms of vibronic interaction has the Mexican-hat-type adiabatic potential energy surface (APES)

$$\varepsilon_{\pm} = \tfrac{1}{2}\omega_E^2\left(Q_\theta^2 + Q_\epsilon^2\right) \pm |V_E|\sqrt{Q_\theta^2 + Q_\epsilon^2} \tag{1}$$

described by Q_θ and Q_ϵ coordinates with a conical intersection at $Q_\theta = Q_\varepsilon = 0$. Here, V_E is the linear vibronic constant, and ω_E is the frequency of the e vibrations in the ground state.

The model Hamiltonian of the linear $E \otimes e$ Jahn-Teller problem is

$$\mathcal{H} = -\frac{\hbar^2}{2}\left(\frac{d^2}{dQ_\theta^2} + \frac{d^2}{dQ_\epsilon^2}\right) + \frac{\omega_E^2}{2}\left(Q_\theta^2 + Q_\epsilon^2\right) + V_E(Q_\theta\hat{\sigma}_x + Q_\epsilon\hat{\sigma}_y) \tag{2}$$

in the basis of current-carrying electronic states $\psi_{1,2} = (\psi_\theta \pm i\psi_\epsilon)/\sqrt{2}$; $\hat{\sigma}_\alpha$ are the Pauli matrices with $\alpha = 0, x, y, z$.

By introducing the cylindrical coordinates $Q_\theta = \rho\cos\varphi$, $Q_\epsilon = \rho\sin\varphi$, the Hamiltonian (2) can be recast in the equivalent form

$$\mathcal{H} = -\frac{\hbar^2}{2}\left[\frac{1}{\rho}\frac{\partial}{\partial\rho}\left(\rho\frac{\partial}{\partial\rho}\right) + \frac{1}{\rho^2}\frac{\partial^2}{\partial\varphi^2}\right]\hat{\sigma}_0 + \frac{\omega_E^2\rho^2}{2}\hat{\sigma}_0 + V_E\rho\begin{pmatrix}0 & e^{-i\varphi}\\ e^{i\varphi} & 0\end{pmatrix}. \tag{3}$$

Eigenstates of this Hamiltonian may be sought in the form $\Psi = \Phi/\sqrt{\rho}$; then, the Hamiltonian $\tilde{\mathcal{H}}$ for $\Phi(\rho,\varphi)$ may be written as

$$\tilde{\mathcal{H}} = \left[-\frac{\hbar^2}{2}\frac{d^2}{d\rho^2} - \frac{\hbar^2}{8\rho^2} + \frac{\hbar^2 L_z^2}{2\rho^2}\right]\hat{\sigma}_0 + \frac{\omega_E^2\rho^2}{2}\hat{\sigma}_0 + V_E\rho\begin{pmatrix}0 & e^{-i\varphi}\\ e^{i\varphi} & 0\end{pmatrix}, \tag{4}$$

where the rotational angular momentum operator $\hat{L}_z = -i\frac{\partial}{\partial\varphi}$ is defined.

Applying the unitary transformation, $\tilde{\mathcal{H}}' = \hat{S}^\dagger\tilde{\mathcal{H}}\hat{S}$, with

$$\hat{S} = \frac{1}{\sqrt{2}}\begin{pmatrix}e^{-i\frac{\varphi}{2}} & e^{-i\frac{\varphi}{2}}\\ e^{i\frac{\varphi}{2}} & -e^{i\frac{\varphi}{2}}\end{pmatrix}, \tag{5}$$

yields the Hamiltonian in the basis of the APES eigenstates

$$\tilde{\mathcal{H}}' = \left[-\frac{\hbar^2}{2}\frac{d^2}{d\rho^2} - \frac{\hbar^2}{8\rho^2} + \frac{\omega_E^2\rho^2}{2}\right]\hat{\sigma}_0 + \frac{\hbar^2}{2\rho^2}\left(\hat{L}_z - \frac{1}{2}\hat{\sigma}_x\right)^2 + V_E\rho\hat{\sigma}_z. \tag{6}$$

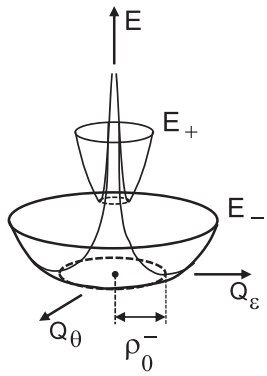

FIG. 1. Adiabatic potential energy surfaces $E_\pm$ of the Jahn-Teller $E \otimes e$ problem. The trough of the lower sheet E_- has a minimum at ρ_0^- resulting from a balance of elastic and JT forces.

The total angular momentum operator, $\hat{J}_z = \hat{L}_z + \frac{1}{2}\hat{\sigma}_z$, consisting of the rotation angular momentum operator $\hat{L}_z$ and the electronic angular momentum operator $\hat{\sigma}_z/2$, commutes with the Hamiltonian (4) and all states may be marked by the half-integer quantum numbers $j = \pm\frac{1}{2}, \pm\frac{3}{2}, \ldots$ [30].

Using the unitary transformation (5) it is straightforward to show that $\hat{J}'_z = \hat{S}^\dagger \hat{J}_z \hat{S} = \hat{L}_z$; then the eigenstate $\Phi(\rho, \varphi)$ of (6) may be factorized into two terms

$$\Phi(\rho, \varphi) = \frac{1}{\sqrt{2\pi}} e^{ij\varphi} \chi(\rho), \tag{7}$$

where a motion along the adiabatic potential trough is described by the φ coordinate of free rotations, while the radial motion along ρ is characterized by the function $\chi(\rho)$. The latter is governed by the Hamiltonian

$$\tilde{\mathcal{H}}_\chi = \left[-\frac{\hbar^2}{2}\frac{d^2}{d\rho^2} + \frac{\hbar^2 j^2}{2\rho^2} + \frac{\omega_E^2 \rho^2}{2} \right] \hat{\sigma}_0 - \frac{\hbar^2 j}{2\rho^2}\hat{\sigma}_x + V_E \rho \hat{\sigma}_z. \tag{8}$$

In the adiabatic approximation the term with $\hat{\sigma}_x$, which mixes the APES sheets, can be neglected, and, as an eventual result, the original Schrödinger equation with the Hamiltonian (3) is transformed into a pair of uncoupled nonlinear equations for the nuclear radial wave function $\chi(\rho)$

$$\left[-\frac{\hbar^2}{2}\frac{d^2}{d\rho^2} + \frac{\hbar^2 j^2}{2\rho^2} + \frac{\omega_E^2 \rho^2}{2} \pm |V_E|\rho \right] \chi(\rho) = E_\pm \chi(\rho). \tag{9}$$

Here the sign $+/-$ serves to distinguish the upper/lower branches of the adiabatic potential. The left-hand side include both the elastic, Jahn-Teller, and centrifugal energies. As has been shown by Slonczewski, on the lower branch of the AP the Jahn-Teller force competes with elastic forces to reach equilibrium (*elastically stabilized motion*). In contrast, on the upper AP branch, the centrifugal force is vital to establish the equilibrium position, but elastic forces are not (*centrifugally stabilized motion*) [31] (see Fig. 1).

Solutions of Eqs. (9) can be expressed in terms of harmonic oscillator wave functions $\chi_n(\rho - \rho_0^\pm)$ $(n = 0, 1, 2, \ldots)$ centered at

$$\rho_0^+ \approx \left(\frac{\hbar^2 j^2}{|V_E|}\right)^{\frac{1}{3}} \left[1 - \frac{\omega_E^2}{3|V_E|} \left(\frac{\hbar^2 j^2}{|V_E|}\right)^{\frac{1}{3}} \right] \tag{10}$$

for the upper AP branch, and at

$$\rho_0^- \approx \frac{|V_E|}{\omega_E^2} \left[1 + \frac{\hbar^2 j^2 \omega_E^2}{|V_E|^4} \right] \tag{11}$$

for the lower one.

Thus, the general solution of the initial Hamiltonian (3) is found to be

$$\Psi_{nj}^\pm(r, \rho, \varphi) = \psi_\pm(r, \varphi)\chi_n\big(\rho - \rho_0^\pm\big) \frac{e^{ij\varphi}}{\sqrt{2\pi\rho}}, \tag{12}$$

where the adiabatic electronic eigenstates are

$$\psi_\pm(r, \varphi) = \frac{1}{\sqrt{2}}\big[e^{-i\frac{\varphi}{2}}\psi_1(r) \pm e^{i\frac{\varphi}{2}}\psi_2(r)\big].$$

To find polarizability of the JT X_3 molecule valid for low temperatures we need low-lying vibronic states only. In our further treatment we assume that the JT stabilization energy $E_{JT} = V_E^2/2\omega_E^2$ is large enough; i.e., the depth of the AP well at the point ρ_0^- is greater than the kinetic energy of the circular motion along the trough and transitions between the lower and upper sheets of the APES may be ignored. As a result, the vibronic energy states are limited to the so-called *rotovibrational spectrum*

$$E_{n,j} = \hbar\omega_E \left(n + \frac{1}{2} \right) + \frac{\hbar^2 j^2}{2\rho_0^{-2}} - E_{JT}, \tag{13}$$

where the quantum numbers j and n specify rotational and radial motions of nuclei, respectively.

Thus, in the regime of strong linear vibronic coupling, the vibrational motion of the nuclei splits the adiabatic potential states into levels lying comparatively close together, $\hbar\omega_E \ll E_{JT}$. These levels, in turn, exhibit a fine splitting into a series of doublet levels of rotational motion with the energy distance $\hbar^2\omega_E^2(2|j| + 1)/4E_{JT}$; i.e., a conventional hierarchy of vibrational spectra in molecules is maintained [4,32].

III. POLARIZABILITY

A calculation of the Casimir-Polder interaction (van der Waals potential) between a molecule with the quantum vacuum comprises the calculation of the dynamic polarizability of the molecule, which is a measure of its response to an electric field oscillating at a frequency ω.

At zero temperature the polarizability of the X_3 molecule in the ground degenerate E state is limited only to transitions between the lowest rotational states with $n = 0$ and $m = \pm\frac{1}{2}, \pm\frac{3}{2}$. The electric dipole interaction with the nuclei does not lead to purely rotational transitions since its matrix elements are nonzero only when $\Delta n = \pm 1$. However, this restriction is removed when the vibronic interaction is taken into account. As a consequence, the purely rotational electric dipole transitions with $n = 0$ become possible due to the nuclear dipole moment.

In the molecular framework the latter can be expressed as

$$\mathbf{D}_n(Q) = Z_E Q_x \mathbf{e}_x + Z_E Q_y \mathbf{e}_y. \tag{14}$$

Here, Z_E is the effective charge of the polar vibrational e mode that produces the dipole moment; $\mathbf{e}$ is the polarization vector of the radiation field.

For the trigonal system with the D_{3h} symmetry of the X_3 molecule, the appropriate symmetrized atomic displacements in terms of Cartesian coordinates read

$$Q_\theta = Q_x = \frac{1}{\sqrt{3}}(x_1 + x_2 + x_3), \tag{15}$$

$$Q_\varepsilon = Q_y = \frac{1}{\sqrt{3}}(y_1 + y_2 + y_3). \tag{16}$$

Since the low-lying part of the vibronic spectrum corresponds to the circular states $\Psi^-_{0\pm\frac{1}{2}}$ and $\Psi^-_{0\pm\frac{3}{2}}$ defined in (12), it is convenient to recast (14) into the equivalent form

$$\mathbf{D}_n(Q) = Z_E Q_+ \mathbf{e}_- + Z_E Q_- \mathbf{e}_+ \tag{17}$$

by introducing the circular basis of the electromagnetic field polarization $\mathbf{e}_\pm = (\mathbf{e}_x \pm i\mathbf{e}_y)/\sqrt{2}$. These radiation circular components are coupled with the nuclei displacements

$$Q_\pm = \frac{1}{\sqrt{2}}(Q_\theta \pm iQ_\epsilon) = \frac{\rho}{\sqrt{2}} e^{\pm i\varphi},$$

which describe clockwise or counterclockwise motion along the circular trough of equal-energy minima on the lower sheet of the APES.

To find appropriate nuclear dipole transitions, the radial vibrations are decomposed as $\rho = \rho_0^- + r$, where ρ_0^- is the radius of the circle at the bottom of the trough (11), and so

$$Q_\pm = \frac{1}{\sqrt{2}}\rho_0^- e^{\pm i\varphi} + \frac{1}{\sqrt{2}} r e^{\pm i\varphi}.$$

(Below, we will omit the upper minus sign in ρ_0 being restricted to the lower APES sheet.) Apparently, the first term gives rise to transitions with $\Delta n = 0$, while the second is related to the change $\Delta n = \pm 1$. Therefore, the relevant dipole transitions at low temperatures in the regime of strong linear vibronic coupling are [33]

$$\langle \Psi^-_{0\pm\frac{1}{2}} | Q_\pm | \Psi^-_{0\mp\frac{1}{2}} \rangle = \langle \Psi^-_{0\pm\frac{3}{2}} | Q_\pm | \Psi^-_{0\pm\frac{1}{2}} \rangle \approx \frac{|V_E|}{\sqrt{2}\omega_E^2}.$$

To find the dynamic polarizability we calculate the expectation value of the nuclear dipole moment operator using the first-order perturbed wave function for the initial ground state

$$|\Psi_0\rangle = c_1 \Psi^-_{0,\frac{1}{2}} + c_2 \Psi^-_{0,-\frac{1}{2}} \tag{18}$$

with $|c_1|^2 + |c_2|^2 = 1$. This approach (for example, see Ref. [34]) leads to the result for the dynamic polarizability

$$\hat{\alpha} = \begin{pmatrix} \alpha_{xx} & \alpha_{xy} & 0 \\ -\alpha_{xy} & \alpha_{xx} & 0 \\ 0 & 0 & 0 \end{pmatrix} \tag{19}$$

with the tensor components

$$\alpha_{xx} = \frac{Z_E^2 \rho_0^2}{4\hbar} \frac{\omega_0}{\omega_0^2 - \omega^2} \tag{20}$$

and

$$\alpha_{xy} = i\frac{Z_E^2 \rho_0^2}{4\hbar}(|c_1|^2 - |c_2|^2)\frac{\omega}{\omega_0^2 - \omega^2}. \tag{21}$$

To obtain an estimate for the frequency of the transition between the neighboring Kramers levels

$$\omega_0 = \frac{1}{\hbar}\left(E_{\pm\frac{3}{2}} - E_{\pm\frac{1}{2}}\right) = \frac{\hbar}{\rho_0^2} \approx \omega_E \left(\frac{\hbar\omega_E}{2E_{JT}}\right),$$

we use the values for the dimensionless JT stabilization energy $E_{JT}/\hbar\omega_E = 2.53$ and the frequency of the E-type vibrations, $\omega_E = 250\,\mathrm{cm}^{-1}$, in the molecule Li_3 [10]. This immediately yields $\omega_0 \approx 49.41\,\mathrm{cm}^{-1}$ (or, equivalently, 1.481 THz) and $E_{JT} = 632.5\,\mathrm{cm}^{-1}$.

The normal coordinate ρ_0 in mass-weighted length units amounts to $\rho_0 = \sqrt{\hbar/\omega_0} \approx 2.668 \times 10^{-20}\,\mathrm{g}^{1/2}\,\mathrm{cm}$. By using the molar mass of Li_3 20.823 g/mol, i.e., the density mass of the Li_3 molecule being $m_n \approx 3.457 \times 10^{-23}$ g, we obtain $\rho_0 \approx 0.454$ Å. The effective nuclear charge for the valence $2s$ electron in lithium is $Z_E \approx 1.279|e| = 6.144 \times 10^{-10}$ esu (see, for example, Ref. [35]).

At last, a measure of absorption intensity is the dimensionless oscillator length

$$f_{\pm\frac{1}{2}\to\pm\frac{3}{2}} = \frac{2m_n\omega_0}{3\hbar} \sum_{\alpha=x,y} \left| \left\langle \pm\frac{1}{2} \middle| Q_\alpha \middle| \pm\frac{3}{2} \right\rangle \right|^2 = \frac{m_n\omega_0\rho_0^2}{3\hbar}, \tag{22}$$

which is approximately equal to 0.332.

IV. CASIMIR INTERACTION

The vacuum fluctuation-induced Casimir-Polder force acting on an atom or molecule in a generic electromagnetic environment depends on the interaction Casimir energy [36]

$$\mathcal{E}_C = -\frac{\hbar}{4\pi}\int_{-\infty}^{\infty} d\xi\, \mathrm{Tr}\{\hat{\alpha}(i\xi)(-i\omega\hat{G})_{\omega=i\xi}\}, \tag{23}$$

which, apart from the found dynamic polarizability, is determined by the system Green function, $\hat{G}(\mathbf{r}, \mathbf{r}', \omega)$, evaluated at imaginary frequencies $\omega = i\xi$ and taken with identical observation and source points, $\mathbf{r} = \mathbf{r}' = \mathbf{r}_0$. (Here, $\mathbf{r}_0$ is a position of the atom or molecule.) The explicit form of $\hat{G}$ for a gyrotropic media half-space is discussed in detail in the Appendix according to Ref. [26], and the final result is given by Eq. (A16).

In this approach, the permittivity $\hat{\varepsilon}(\omega)$ of the metal half-space is modeled by the gyrotropic permittivity of a plasma in the external static magnetic field $\mathbf{B}$ [26]. If the ac electric field $\mathbf{E}(t) = \mathbf{E}_0 e^{-i\omega t}$ is applied, the electrons start to oscillate with the frequency ω, so that the velocity of the oscillation lags $\pi/2$ behind the oscillation of $\mathbf{E}(t)$. Simultaneously, in the plane perpendicular to $\mathbf{B}$ the electron motion presents superposition of the circular motion at the cyclotron frequency ω_c with an oscillation at the frequency ω [37].

This model results in the following tensor form,

$$\hat{\varepsilon}(\omega) = \begin{pmatrix} \varepsilon_t(\omega) & 0 & i\varepsilon_g(\omega) \\ 0 & \varepsilon_a(\omega) & 0 \\ -i\varepsilon_g(\omega) & 0 & \varepsilon_t(\omega) \end{pmatrix}, \tag{24}$$

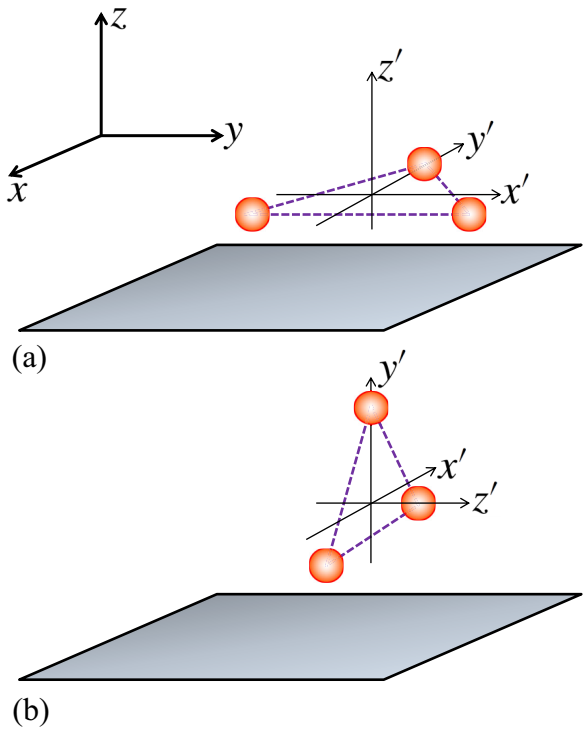

FIG. 2. Horizontal (a) and vertical (b) orientations of the molecule plane relative to the interface surface.

where the components depend on the electron plasma frequency ω_p,

$$\varepsilon_t(\omega) = 1 - \frac{\omega_p^2}{\omega^2 - \omega_c^2}, \quad \varepsilon_a(\omega) = 1 - \frac{\omega_p^2}{\omega^2},$$
$$\varepsilon_g(\omega) = \frac{\omega_c \omega_p^2}{\omega(\omega_c^2 - \omega^2)}. \tag{25}$$

A. Casimir-Polder coupling

A coupling between the Jahn-Teller X_3 molecule and the gyrotropic material half-space mediated by the photon field is expected to depend on the orientation of the molecular axes (x', y', z') with respect to the interface coordinate axes (x, y, z). Below, we focus on the two cases (i) when the molecular plane is parallel to the interface plane and (ii) when these planes are mutually perpendicular.

1. Horizontal orientation

The orientation of the molecular axes with respect to the interface reference frame is determined by the rotation $\mathbf{r} = \hat{R}^H \mathbf{r}'$ with the matrix [see Fig. 2(a)]

$$\hat{R}^H = \begin{pmatrix} 0 & -1 & 0 \\ 1 & 0 & 0 \\ 0 & 0 & 1 \end{pmatrix}.$$

The components of the polarization tensor in the two frames are related by

$$\alpha'_{mn} = \alpha_{ij} R^H_{im} R^H_{jn}, \tag{26}$$

where α'_{ij} are determined by Eqs. (19)–(21).

Some straightforward algebra leads to the expression

$$\mathrm{Tr}\{\hat{\alpha}(\omega)[-i\omega \hat{G}_{EE}(\omega)]\} = \frac{Z_E^2 \rho_0^2}{64\varepsilon_0 \hbar \pi^2 d^3} \frac{\omega_0}{(\omega_0^2 - \omega^2)} \times \int_0^{2\pi} d\theta \, \frac{a_\theta \omega_\theta^2}{\omega_\theta^2 - \omega^2}, \tag{27}$$

in which the results (A12) and (A16) are accounted for. Here, d is a distance of the molecule center of mass with respect to the interface plane, and ω_θ is the frequency of the surface plasmon polaritons (SPPs) determined by Eq. (A8). The dispersion of these modes arises from the dependence of their frequencies on the angle θ between the in-plane wave vector direction of the propagating SPP modes and the direction of the static magnetic field inside the gyrotropic medium. The positive θ-dependent factor a_θ is given by Eq. (A14). Note specifically that the dyadic Green function $\hat{G}$, incorporating, in general, both electric and magnetic parts, is reduced to the purely electric constituent $\hat{G}_{EE}$ in the quasistatic approximation, which is relevant for small d (see Appendix).

Performing in Eq. (23) transition to integration over the imaginary frequency axis, $\omega = i\xi$, one finds the Casimir-Polder energy in the horizontal geometry

$$\begin{aligned} \mathcal{E}_C^H &= \frac{i\hbar}{4\pi} \int_{-i\infty}^{i\infty} d\omega \, \mathrm{Tr}\{\hat{\alpha}(\omega)[-i\omega \hat{G}_{EE}(\omega)]\} \\ &= \frac{i Z_E^2 \rho_0^2 \omega_0}{256\varepsilon_0 \pi^3 d^3} \int_0^{2\pi} d\theta \, a_\theta \omega_\theta^2 \\ &\quad \times \int_{-i\infty}^{i\infty} d\omega \, \frac{1}{(\omega_0^2 - \omega^2)} \frac{1}{(\omega_\theta^2 - \omega^2)} \\ &= -\frac{Z_E^2 \rho_0^2}{256\varepsilon_0 \pi^2 d^3} \int_0^{2\pi} d\theta \, \frac{a_\theta \omega_\theta}{\omega_\theta + \omega_0}. \end{aligned} \tag{28}$$

In the above, the integral

$$\int_{-i\infty}^{i\infty} d\omega \, \frac{1}{(\omega_0^2 - \omega^2)} \frac{1}{(\omega_\theta^2 - \omega^2)} = \frac{i\pi}{\omega_0 \omega_\theta (\omega_0 + \omega_\theta)} \tag{29}$$

is exploited.

As the negative sign shows, $\mathcal{E}_C^H$ describes attraction between the JT X_3 molecule and the surface of the gyrotropic media. The strength of the interaction is determined by the factor $Z_E^2 \rho_0^2 / (256\varepsilon_0 \pi^2 d^3)$, which is of order 2.42×10^{-11} eV for the trimer Li_3 at $d = 100$ nm. Note that the expression for $\mathcal{E}_C^H$ is ground-state independent; therefore twofold degeneracy of the ground state is not lifted and rotational symmetry remains unbroken [3].

2. Vertical orientation

A detailed calculation of the Casimir-Polder energy for the perpendicular relative orientation of the molecular and the interface planes may be performed in the same vein.

The matrix

$$\hat{R}^V = \begin{pmatrix} -1 & 0 & 0 \\ 0 & 0 & 1 \\ 0 & 1 & 0 \end{pmatrix}$$

specifies the mapping between the components of $\mathbf{r}$ and $\mathbf{r}'$, i.e. $\mathbf{r} = \hat{R}^V \mathbf{r}'$ [see Fig. 2(b)].

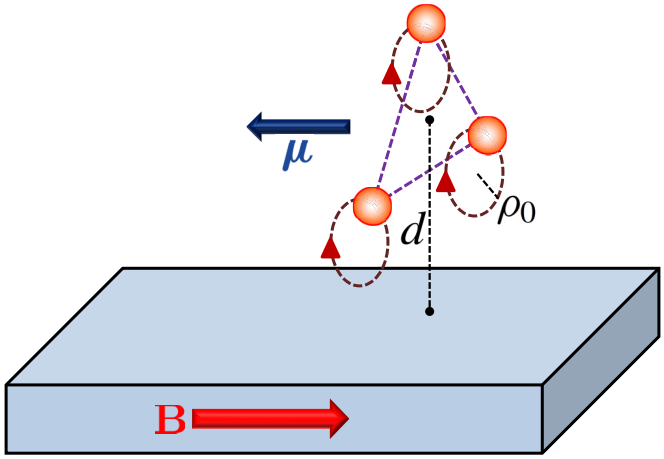

FIG. 3. Magnetic moment $\boldsymbol{\mu}$ (blue arrow) created by the nuclei clockwise rotation due to broken rotational symmetry is oppositely aligned with the magnetic field **B** (red arrow) inside the gyrotropic medium.

It is convenient to switch to the interface plane coordinate frame to find

$$\begin{aligned}&\mathrm{Tr}\{\hat{\alpha}(\omega)[-i\omega\hat{G}_{EE}(\omega)]\}\\&=\frac{Z_E^2\rho_0^2}{64\hbar\varepsilon_0\pi^2 d^3}\frac{\omega_0}{\omega_0^2-\omega^2}\int_0^{2\pi}d\theta(1+\cos^2\theta)\frac{a_\theta\omega_\theta^2}{\omega_\theta^2-\omega^2}\\&+\frac{Z_E^2\rho_0^2}{32\hbar\varepsilon_0\pi^2 d^3}(|c_1|^2-|c_2|^2)\frac{\omega^2}{\omega_0^2-\omega^2}\\&\times\int_0^{2\pi}d\theta\cos\theta\frac{a_\theta\omega_\theta}{\omega_\theta^2-\omega^2}.\end{aligned}\tag{30}$$

Making use of the integral (29) along with

$$\int_{-i\infty}^{i\infty}d\omega\,\frac{\omega^2}{(\omega_0^2-\omega^2)}\frac{1}{(\omega_\theta^2-\omega^2)}=-\frac{i\pi}{\omega_\theta+\omega_0}$$

in integration of (30) over the imaginary frequencies leads to the following result for the Casimir-Polder energy in the vertical geometry,

$$\begin{aligned}\mathcal{E}_C^V=&-\frac{Z_E^2\rho_0^2}{256\varepsilon_0\pi^2 d^3}\int_0^{2\pi}d\theta(1+\cos^2\theta)\frac{a_\theta\omega_\theta}{\omega_\theta+\omega_0}\\&+\frac{Z_E^2\rho_0^2}{128\varepsilon_0\pi^2 d^3}(|c_1|^2-|c_2|^2)\int_0^{2\pi}d\theta\cos\theta\frac{a_\theta\omega_\theta}{\omega_\theta+\omega_0}.\end{aligned}\tag{31}$$

It is clearly seen that the ground-state Kramers degeneracy is lifted, $|c_1|=0$ and $|c_2|=1$, because of the energy gain associated with the second term. Apart from this contribution, the ground-state independent term turns out to be less than the analogous result (28) for the horizontal orientation of the X_3 molecule.

The initial doubly degenerate eigenfunctions are related to two possible directions of nuclei rotations, i.e., in the clockwise or counterclockwise manner around their local axes. This rotational symmetry will be broken by the quantum vacuum fluctuations.

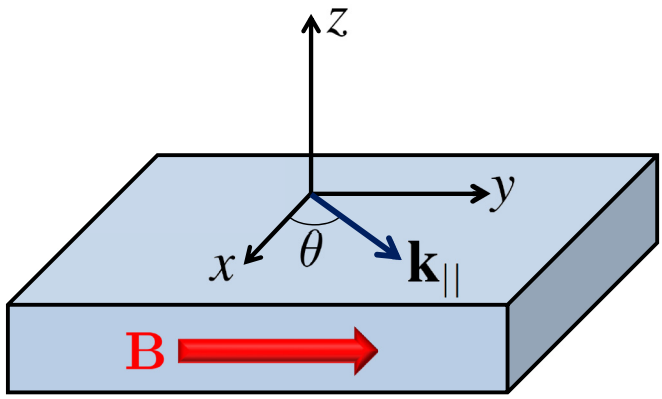

FIG. 4. Geometry of the gyrotropic half-space. The surface plasmon polariton propagates within the xy plane along the direction of the wave vector $\mathbf{k}_{||}$ given by the polar angle θ. A static magnetic field inside the media is oriented along the y axis.

V. MAGNETIC MOMENT AND BERRY PHASE DUE TO BROKEN ROTATIONAL SYMMETRY

A. Magnetic moment

A direct consequence of rotational symmetry breaking is the appearance of a magnetic moment in the X_3 molecule which is intimately associated with nuclei motion. Below, the issue is addressed in the semiclassical scheme proposed in Ref. [3].

To start with, one constructs the effective Hamiltonian

$$\hat{H}_{\mathrm{eff}}=\sum_j E_j|j\rangle\langle j|\tag{32}$$

defined in the restricted Hilbert space of the low-lying rotational states with $j=\pm\frac{1}{2},\pm\frac{3}{2}$ and the appropriate eigenvalues $E_{\pm\frac{1}{2}}=0$, $E_{\pm\frac{3}{2}}=\hbar\omega_0$.

The angular momentum due to nuclei circular motion is

$$\hat{\mathbf{L}}=[\hat{\mathbf{Q}}\times\hat{\mathbf{P}}]=(\hat{Q}_x\hat{P}_y-\hat{Q}_y\hat{P}_x)\mathbf{e}_z,\tag{33}$$

where all components are given in the molecular reference frame.

Derivation of the nuclei momentum **P** relies on solving the equation of motion

$$\frac{\hat{P}_\alpha}{m_n}=\frac{d\hat{Q}_\alpha}{dt}=\frac{i}{\hbar}[\hat{H}_{\mathrm{eff}},\hat{Q}_\alpha],\quad(\alpha=x,y),\tag{34}$$

where m_n is the molecule mass.

Using the matrix representation for the circular coordinates in the basis $\{|-\frac{3}{2}\rangle,|-\frac{1}{2}\rangle,|\frac{1}{2}\rangle,|\frac{3}{2}\rangle\}$

$$\begin{aligned}\hat{Q}_+&=\frac{\rho_0}{\sqrt{2}}\begin{pmatrix}0&0&0&0\\1&0&0&0\\0&1&0&0\\0&0&1&0\end{pmatrix},\\\hat{Q}_-&=\frac{\rho_0}{\sqrt{2}}\begin{pmatrix}0&1&0&0\\0&0&1&0\\0&0&0&1\\0&0&0&0\end{pmatrix},\end{aligned}\tag{35}$$

it is easy to establish that

$$[\hat{H}_{\text{eff}}, \hat{Q}_x] = \frac{i}{2}\hbar\omega_0\rho_0\,(\hat{\sigma}_z \otimes \hat{\sigma}_y), \tag{36}$$

$$[\hat{H}_{\text{eff}}, \hat{Q}_y] = \frac{i}{2}\hbar\omega_0\rho_0\,(\hat{\sigma}_z \otimes \hat{\sigma}_x), \tag{37}$$

where $\otimes$ stands for the direct product of the Pauli matrices σ_α ($\alpha = x, y, z$).

From Eq. (33) it is straightforward to show that

$$\hat{L}_z = -I_n\omega_0\,(\hat{\sigma}_z \otimes \hat{\sigma}_0), \tag{38}$$

where $I_n = \frac{1}{2}m_n\rho_0^2$ is the moment of inertia of the JT X_3 molecule.

Following the classical argument, a magnetic dipole moment generated by rotation of a charge Z_E of mass m_n in an orbit of the radius ρ_0 in the xy plane, $\mu_z = Z_E\omega_0\rho_0^2/2$, is proportional to the angular momentum $L_z = m_n\omega_0\rho_0^2$ through the relation $\mu_z = \gamma_n L_z$, where the gyromagnetic ratio is introduced, $\gamma_n = Z_E/2m_n$.

This immediately implies that the magnetic moment operator due to nuclei rotation is given by

$$\hat{\mu}_z = -\gamma_n I_n\omega_0\,(\hat{\sigma}_z \otimes \hat{\sigma}_0), \tag{39}$$

whose expectation value for the ground state takes the form

$$\langle\Psi_0|\hat{\mu}_z|\Psi_0\rangle = \tfrac{1}{4}Z_E\omega_0\rho_0^2(|c_1|^2 - |c_2|^2). \tag{40}$$

When there is the twofold degeneracy of the ground state, $|c_1|^2 = |c_2|^2 = 1/2$, the magnetic moment is absent, but when the Kramers degeneracy is lifted, $|c_1|^2 = 0$ and $|c_2|^2 = 1$, the magnetic moment $\mu_z = -Z_E\omega_0\rho_0^2/4$, which is of order $0.03\mu_N$ in Li_3 trimer, appears. (Here, $\mu_N = 5.051 \times 10^{-27}$ A m^2 is the nuclear magneton.) For comparison, the magnetic moment of three equivalent $I = 1$ nuclei of ^{6}Li isotopes, which is detectable in the ESR experiment via the small hyperfine interaction [17], equals $3g_0 I\mu_N \approx 6.00846\mu_N$, where $g_0 \approx 2.00282$. The sign minus means that the induced magnetic moment and the magnetic field inside the gyrotropic media are oppositely directed; i.e., Lenz's law is retained. The effect can rightly be called *diamagnetsim mediated by vacuum fluctuations* (Fig. 3).

It should be understood that there is no direct Zeeman interaction of the magnetic field **B**, which operates inside the metal half-space, with electron and nuclear magnetic moments of the molecule located in vacuum, where the magnetic field is absent. Even though **B** determines the magnitude of the Casimir-Polder coupling, it just triggers time-reversal symmetry breaking inside the molecule when the field strength does not matter. In addition, the direct Zeeman interaction could not be able to govern spatial orientation of the molecule.

Finally, we consider what happens when the JT X_3 molecule is positioned near a reciprocal substrate, e.g., a standard metal surface, whose interaction tensor is given by [3]

$$-i\omega\hat{G}_{EE}(\omega) = \frac{1}{32\pi d^3}\frac{\varepsilon(\omega)-1}{\varepsilon(\omega)+1}\begin{pmatrix}1&0&0\\0&1&0\\0&0&2\end{pmatrix}. \tag{41}$$

Here,

$$\frac{\varepsilon(\omega)-1}{\varepsilon(\omega)+1} = \frac{\omega_{\text{sp}}^2}{\omega_{\text{sp}}^2 - \omega^2}, \tag{42}$$

where $\omega_{\text{sp}} = \omega_p/\sqrt{2}$ is the surface plasmon resonance.

Starting with the horizontal orientation of the molecule plane and making subsequent rotation by an angle θ around the reference x axis with the help of the matrix

$$\hat{R}_x = \begin{pmatrix}1&0&0\\0&\cos\theta&-\sin\theta\\0&\sin\theta&\cos\theta\end{pmatrix}, \tag{43}$$

the Casimir-Polder energy can be evaluated similarly to (28). The result is

$$\mathcal{E}_C = -\frac{1}{64\pi d^3}\left(\frac{Z_E\rho_0}{2}\right)^2\frac{\omega_{\text{sp}}}{\omega_{\text{sp}}^2-\omega^2}\left(1+\frac{1}{2}\sin^2\theta\right), \tag{44}$$

which coincides with Eq. (27) in Ref. [3], if only chiral (circularly polarized) transitions count.

Clearly, the orientation of the molecule plane perpendicular to the substrate ($\theta = \pi/2$) becomes energetically favourable. However, the new equilibrium position does not lift the ground-state degeneracy, and, consequently, there is no magnetic moment induced by a broken time-reversal symmetry.

B. Berry phase

In order to gain insight into how the broken rotational symmetry is related with a molecular geometric phase, it is necessary to examine the Berry phase for a rotational loop in nuclear configuration space, where φ varies over nonzero multipliers of 2π.

The Berry connection associated with the rotational motions of nuclei of the $E \otimes e$ JT problem, when radial displacements are ignored, is determined by

$$A_\varphi = i\langle\Psi_0(\mathbf{r},\rho,\varphi)|\,\nabla_\varphi\Psi_0(\mathbf{r},\rho,\varphi)\rangle.$$

Here, the vibrational ground state (18) is involved.

A direct calculation leads to the result

$$A_\varphi = \frac{1}{2\rho_0}(|c_2|^2 - |c_1|^2).$$

The Berry phase γ is then determined as the circulation of $\mathbf{A}$ along the closed path $\mathcal{C}$ around the z axis of the nuclei coordinate space [38]

$$\gamma = \oint_{\mathcal{C}}\mathbf{A}\cdot d\mathbf{Q} = \int_0^{2\pi}A_\varphi\rho_0 d\varphi = \pi(|c_2|^2 - |c_1|^2).$$

Thus, the emergence of the nontrivial molecular geometric phase π due to the lifted Kramers degeneracy ($|c_2|^2 = 1$ and $|c_1|^2 = 0$) is another concomitant effect of the broken rotational symmetry.

VI. CONCLUSIONS

As a summary, this paper investigates peculiarities of the Casimir-Polder interaction between the Jahn-Teller X_3 molecule with the linear $E \otimes e$ problem and the interface of a gyrotropic medium. Our results demonstrate that the vertical orientation of the molecule plane with respect to the interface

surface is more energetically favorable than the corresponding horizontal orientation. This effect becomes possible due to the rotational symmetry breaking mechanism provided by the Casimir-Polder coupling, which lifts degeneracy of circular motion of the JT molecule nuclei. Moreover, we demonstrate that a direct consequence of the rotational symmetry breaking is the appearance of the orbital magnetic moment and accumulation of the topological Berry phase. Remarkably, directions of the induced magnetic moment and the magnetic field inside the gyrotropic medium are oppositely aligned. It makes it possible to achieve collective orientational coherence of a cloud of such molecules placed close to the gyrotropic medium. We believe that this property can be potentially used to design a spin filter device on the base of the Jahn-Teller molecules.

Furthermore, we anticipate that obvious correlation between a nuclei motion, magnetic polarization, and Berry phase accumulation may contribute to our understanding of chiral-induced spin selectivity (CISS) [39]. In this regard, the work [40] should be noted, where dynamically generated spin polarization in chiral molecules interfaced with a metallic surface was reported. Specifically, it was argued that the CISS is an excited state phenomenon which appears in the transient regime immediately after coupling of a chiral molecule with a metallic surface. In the presence of electron-vibration interaction these transient spin fluctuations become stable and develop into finite spin polarization in the stationary limit. Nuclear vibrations of the molecule facilitates angular momentum transfer between states which form the ground state to maintain the nonvanishing spin polarization. A close idea was put forward in Ref. [41], where the authors contend that CISS may arises when nuclear motion becomes entangled with spin-dependent electronic dynamics. Particularly, they hypothesized that nonadiabatic dynamics in the presence of degenerate electronic state will produce a nonzero Berry curvature which can be transformed into an effective magnetic field. The latter may be crucial as far as creating chiral-induced spin separation.

At last, Ref. [42] should be mentioned, where a possible *static* scenario of CISS was analyzed on the basis of the pseudo-Jahn-Teller Hamilonian for a chiral molecule with C_3 symmetry. In this model a broken chiral symmetry is put into parameters of the pseudo-JT Hamiltonian, which should be considered together with the spin-orbit interaction. Elimination of the nuclear vibronic coordinates results in an effective Hamiltonian with spin-dependent energy spectrum of an electron injected into the molecule [43–46].

ACKNOWLEDGMENTS

J.K. and A.S.O. thank Hiroshi M. Yamamoto for discussions in the early stage of the work. The research funding from the Ministry of Science and Higher Education of the Russian Federation (Ural Federal University Program of Development within the Priority-2030 Program) is gratefully acknowledged. A.S.O. thanks the Ministry of Science and Higher Education of the Russian Federation, Project No. FEUZ-2023-0017. J.K. acknowledges support from Japan Society for the Promotion of Science (JSPS) through a Grant in-Aid for Scientific Research (B) (Grant No. 21H01032), and Joint Research by Institute for Molecular Science (IMS program No. 23IMS1101).

APPENDIX: DYADIC GREEN FUNCTION

The dyadic Green function approach allows us to derive the electric field $\mathbf{E}(\mathbf{r})$ emitted by a classical dipole with electric dipole moment $\mathbf{p}$ located at the point $\mathbf{r}_0$. The electromagnetic field in the vacuum is the superposition of the primary field ($\mathbf{E}^p$) and the scattered field ($\mathbf{E}^s$).

The primary field is given by $\mathbf{E}^p(\mathbf{r}) = -i\omega\hat{G}^{(p)}_{EE}(\mathbf{r}-\mathbf{r}_0)\mathbf{p}$, where the dyadic Green function in a vacuum [47]

$$-i\omega\hat{G}^{(p)}_{EE}(\mathbf{r}-\mathbf{r}_0) = \frac{1}{\epsilon_0}[\hat{I}k^2 + \nabla\nabla]g(\mathbf{r}-\mathbf{r}_0) \tag{A1}$$

is expressed via the scalar Green function

$$g(\mathbf{r}-\mathbf{r}_0) = \frac{e^{ik_0|\mathbf{r}-\mathbf{r}_0|}}{4\pi|\mathbf{r}-\mathbf{r}_0|}.$$

Here, the source point $\mathbf{r}_0 = (0, 0, d)$ is defined via the distance d of the dipole with respect to the interface plane ($z = 0$).

The scalar Green function may be rewritten as an integral summation of plane waves

$$\frac{e^{ik_0|\mathbf{r}-\mathbf{r}_0|}}{4\pi|\mathbf{r}-\mathbf{r}_0|} = \int_{-\infty}^{\infty}\int_{-\infty}^{\infty}\frac{dk_x dk_y}{(2\pi)^2}\frac{e^{ik_x x + ik_y y - \gamma_0|z-d|}}{2\gamma_0}$$

with $\gamma_0 = \sqrt{k_x^2 + k_y^2 - k_0^2}$ and $k_0 = \omega/c$, where the Weyl formula for the plane-wave expansion of a spherical wave is used [47].

A similar representation for the scattering part of the Green function may be derived via the Sommerfield-type integral [26]. However, it is often more convenient to specify $\hat{G}^{(s)}_{EE}$ using the expansion of the dyadic Green function in the natural electromagnetic modes [48]

$$\mathbf{F}_{n\mathbf{k}} = \begin{pmatrix}\mathbf{E}_{n\mathbf{k}}\\ \mathbf{H}_{n\mathbf{k}}\end{pmatrix}.$$

They are normalized

$$\frac{1}{2}\int d\mathbf{r}\,\mathbf{F}^*_{n\mathbf{k}}(\mathbf{r})\frac{\partial}{\partial\omega}[\omega\hat{M}]\mathbf{F}_{n\mathbf{k}}(\mathbf{r}) = 1 \tag{A2}$$

with the factor including the material matrix

$$\hat{M}(\omega) = \begin{pmatrix}\hat{\varepsilon}(\omega) & \hat{0}\\ \hat{0} & \mu_0\hat{I}\end{pmatrix}.$$

The dispersive permittivity of the molecule environment is defined separately in the free space and in the media half-space [3]

$$\hat{\varepsilon}(\omega) = \varepsilon_0\begin{cases}\hat{I}, & z > 0 \quad \text{(vacuum)},\\ \hat{\epsilon}(\omega), & z < 0 \quad \text{(media)}.\end{cases}$$

In the above, $\hat{I}$ is the 3×3 identity matrix and the medium is assumed to be nonmagnetic.

The dyadic Green function can be decomposed as [26,49]

$$\hat{G}^{(s)}(\mathbf{r},\mathbf{r}_1,\omega) = \hat{G}^{+}(\mathbf{r},\mathbf{r}_1,\omega) + \hat{G}^{-}(\mathbf{r},\mathbf{r}_1,\omega) - \frac{i}{\omega}\hat{M}^{-1}_{\infty}\delta(\mathbf{r}-\mathbf{r}_1), \tag{A3}$$

where the positive $\hat{G}^{+}$ and the negative $\hat{G}^{-}$ frequency parts are expanded into the normal modes

$$-i\omega\hat{G}^{+}(\mathbf{r},\mathbf{r}_1,\omega)=\sum_{\omega_{n\mathbf{k}}>0}\frac{\omega_{n\mathbf{k}}}{2}\frac{1}{\omega_{n\mathbf{k}}-\omega}\mathbf{F}_{n\mathbf{k}}(\mathbf{r})\otimes\mathbf{F}^{*}_{n\mathbf{k}}(\mathbf{r}_1), \tag{A4}$$

$$-i\omega\hat{G}^{-}(\mathbf{r},\mathbf{r}_1,\omega)=\sum_{\omega_{n\mathbf{k}}>0}\frac{\omega_{n\mathbf{k}}}{2}\frac{1}{\omega_{n\mathbf{k}}+\omega}\mathbf{F}^{*}_{n\mathbf{k}}(\mathbf{r})\otimes\mathbf{F}_{n\mathbf{k}}(\mathbf{r}_1). \tag{A5}$$

Here, $\omega_{n\mathbf{k}}$ are the frequencies of the normal modes. Note that since the δ-function term in (A3) is related with the self-action and does not contribute to the Casimir-Polder force, it may be ignored below.

In what follows we examine the mechanism of coupling between the JT X_3 molecule and the metallic surface in which the fluctuation-induced force is driven by surface plasmon polaritons (SPPs). A detailed analysis of these excitations may be found in Ref. [26]; below we give just a brief review of SPP characteristics necessary to calculate the Casimir-Polder interaction.

A search of the natural electromagnetic modes is performed in the quasistatic approximation when the electromagnetic wavelength c/ω is assumed to be large compared with the distance d. It makes it possible to choose the purely electric fields $\mathbf{E}_{n\mathbf{k}}=-\nabla\phi_{n\mathbf{k}}$ and $\mathbf{H}_{n\mathbf{k}}\approx\mathbf{0}$, where the electric potential may be obtained from the Maxwell equation $\mathrm{div}[\hat{\varepsilon}(\omega)\nabla\phi_{n\mathbf{k}}]=0$, where $\hat{\varepsilon}(\omega)$ is explicitly determined by Eqs. (24) and (25).

The scalar potential is given in terms of the evanescent waves

$$\varphi(\mathbf{r})=\frac{A_{\mathbf{k}_{||}}}{\sqrt{S}}e^{i(k_x x+k_y y)}\begin{cases}e^{-k_{||}z} & (z>0),\\ e^{\tilde{k}_{||}z} & (z<0),\end{cases} \tag{A6}$$

with $k_{||}=\sqrt{k_x^2+k_y^2}$ and $\tilde{k}_{||}=\sqrt{k_x^2+\frac{\varepsilon_a}{\varepsilon_t}k_y^2}$. Here, S is the interface area; the normalization parameter $A_{\mathbf{k}_{||}}$ will be defined below.

The frequency of the surface plasmon polaritons may be derived from the boundary condition that normal components of the electric displacement $\mathbf{D}$ are continuous at the interface if the surface charge is zero. Moreover, due account must be taken of the fact that the presence of the static magnetic field introduces a space anisotropy in the electron plasma and, as a consequence, it is convenient to introduce the parametrization in terms of the angle θ within the interface plane (Fig. 4)

$$k_x=k_{||}\cos\theta,\quad k_y=k_{||}\sin\theta. \tag{A7}$$

The resonance frequencies are then given by

$$\omega_\theta=\frac{1}{2}\omega_c\cos\theta+\left[\frac{\omega_p^2}{2}+\frac{\omega_c^2}{4}\left(1+\sin^2\theta\right)\right]^{\frac{1}{2}}. \tag{A8}$$

The normalization coefficient is determined from the condition (A2),

$$|A_{\mathbf{k}_{||}}|^2=\frac{2}{\varepsilon_0}\left[k_{||}+\frac{\Lambda\left(\omega_\theta,\omega_c,\omega_p\right)}{2\tilde{k}_{||}}\right]^{-1}, \tag{A9}$$

where

$$\Lambda(\omega_\theta,\omega_c,\omega_p)=\left(k_x^2+\tilde{k}_{||}^2\right)\frac{\partial}{\partial\omega}\{\omega\varepsilon_t(\omega)\}\Big|_{\omega=\omega_\theta}+k_y^2\frac{\partial}{\partial\omega}\{\omega\varepsilon_a(\omega)\}\Big|_{\omega=\omega_\theta}+2k_x\tilde{k}_{||}\frac{\partial}{\partial\omega}\{\omega\varepsilon_g(\omega)\}\Big|_{\omega=\omega_\theta}. \tag{A10}$$

In general, Eqs. (A3)–(A5) determine a 6×6 tensor of the electric and magnetic dyadic Green functions

$$\hat{G}=\begin{pmatrix}\hat{G}_{EE} & \hat{G}_{EH}\\ \hat{G}_{HE} & \hat{G}_{HH}\end{pmatrix}.$$

Apparently, this tensor is reduced to the purely electric 3×3 tensor $\hat{G}_{EE}$ in the quasistatic approximation.

To specify its form, one starts with

$$-i\omega\hat{G}^{+}_{EE}(\mathbf{r},\mathbf{r}',\omega)=\sum_{\mathbf{k}_{||}}\frac{\omega_{\mathbf{k}_{||}}}{2}\frac{1}{\omega_{\mathbf{k}_{||}}-\omega}\nabla\varphi_{\mathbf{k}}(\mathbf{r})\otimes\nabla'\varphi^{*}_{\mathbf{k}}(\mathbf{r}'), \tag{A11}$$

where $\omega_{\mathbf{k}_{||}}$ are frequencies of the normal modes, which are nothing but the SPP resonance frequencies ω_θ.

Replacing summation over $\mathbf{k}_{||}$ by integration and taking the limit $\mathbf{r}\to\mathbf{r}'$ with $z=z'=d$, one has to evaluate

$$-i\omega\hat{G}^{+}_{EE}(\mathbf{r},\mathbf{r},\omega)=\frac{1}{(2\pi)^2}\iint dk_x dk_y|A_{\mathbf{k}_{||}}|^2\frac{\omega_\theta}{2}\frac{1}{\omega_\theta-\omega}\times\left(i\mathbf{k}_{||}-k_{||}\mathbf{e}_z\right)\otimes\left(i\mathbf{k}_{||}-k_{||}\mathbf{e}_z\right)^{*}e^{-2k_{||}d}.$$

Introducing the θ-dependent dimensionless tensor

$$\hat{\Gamma}(\theta)=\frac{1}{k_{||}^2}(i\mathbf{k}_{||}-k_{||}\mathbf{e}_z)\otimes\left(i\mathbf{k}_{||}-k_{||}\mathbf{e}_z\right)^{*}=\begin{pmatrix}\cos^2\theta & \sin\theta\cos\theta & -i\cos\theta\\ \sin\theta\cos\theta & \sin^2\theta & -i\sin\theta\\ i\cos\theta & i\sin\theta & 1\end{pmatrix} \tag{A12}$$

and by changing to polar coordinates, one obtains

$$-i\omega\hat{G}^{+}_{EE}(\mathbf{r},\mathbf{r},\omega)=\frac{1}{32\pi^2\varepsilon_0 d^3}\int_0^{2\pi}d\theta\frac{a_\theta\omega_\theta}{\omega_\theta-\omega}\hat{\Gamma}(\theta), \tag{A13}$$

where the positive $k_{||}$-independent factor is defined as

$$a_\theta=\left|A_{\mathbf{k}_{||}}\right|^2\varepsilon_0 k_{||} \tag{A14}$$

and the elementary integral $\int_0^\infty dk_{||}k_{||}^2e^{-2k_{||}d}=2/(2d)^3$ is exploited.

A similar path is followed to determine

$$-i\omega\hat{G}^{-}_{EE}(\mathbf{r},\mathbf{r},\omega)=\frac{1}{32\pi^2\varepsilon_0 d^3}\int_0^{2\pi}d\theta\frac{a_\theta\omega_\theta}{\omega_\theta+\omega}\hat{\Gamma}^{*}(\theta). \tag{A15}$$

According to (A3), the scattered part of the equal-position dyadic Green function for the gyrotropic media is then

$$-i\omega\hat{G}^{(s)}_{EE}(\mathbf{r},\mathbf{r},\omega)=\frac{1}{32\pi^2\varepsilon_0 d^3}\int_0^{2\pi}d\theta\,a_\theta\omega_\theta\times\left[\frac{\hat{\Gamma}(\theta)}{\omega_\theta-\omega}+\frac{\hat{\Gamma}^{*}(\theta)}{\omega_\theta+\omega}\right]. \tag{A16}$$

[1] H. G. B. Casimir and D. Polder, Phys. Rev. **73**, 360 (1948).
[2] F. Intravaia, C. Henkel, and M. Antezza, Fluctuation-induced forces between atoms and surfaces: The Casimir-Polder interaction, in D. Dalvit, P. Milonni, D. Roberts, and F. da Rosa (editors), *Casimir Physics, Lecture Notes in Physics*, Vol. 834 (Springer, Berlin, 2011).
[3] M. G. Silveirinha, Phys. Rev. B **100**, 165146 (2019).
[4] I. B. Bersuker, *Jahn-Teller Effect* (Cambridge University Press, Cambridge, 2006).
[5] I. B. Bersuker and V. Z. Polinger, *Vibronic Interactions in Molecules and Crystals* (Springer, Berlin, 1989).
[6] R. Renner, Z. Phys. **92**, 172 (1934).
[7] H. Hettema, *Quantum Chemistry: Classic Scientific Papers*, World Scientific Series in 20th Century Chemistry (World Scientific, Singapore, 2000).
[8] P. Garcia-Fernandez and I. B. Bersuker, Int. J. Quantum Chem. **112**, 3025 (2012).
[9] W. Hermoso, Y. Liu, and I. B. Bersuker, J. Chem. Theory Comput. **10**, 4377 (2014).
[10] J. L. Martins, R. Car, and J. Buttet, J. Chem. Phys. **78**, 5646 (1983).
[11] R. Folman, P. Krüger, J. Schmiedmayer, J. Denschlang, and G. Henkel, Adv. At. Mol. Opt. Phys. **48**, 263 (2002).
[12] J. Fortágh and C. Zimmermann, Rev. Mod. Phys. **79**, 235 (2007).
[13] W. H. Gerber and E. Schumacher, J. Chem. Phys. **69**, 1692 (1978).
[14] H.-G. Krämer, M. Keil, C. B. Suarez, W. Demtröder, and W. Meyer, Chem. Phys. Lett. **299**, 212 (1999).
[15] J.-P. Wolf, G. Delacrétaz, and L. Wöste, Phys. Rev. Lett. **63**, 1946 (1989).
[16] R. O. Jones, in *Electronic Density Functional Theory: Recent Progress and New Directions* (Plenum, New York, 1998), p. 349.
[17] D. A. Garland and D. M. Lindsay, J. Chem. Phys. **78**, 2813 (1983).
[18] D. T. Butcher, S. Y. Buhmann, and S. Scheel, New J. Phys. **14**, 113013 (2012).
[19] P. Barcellona, R. Passante, L. Rizzuto, and S. Y. Buchmannn, Phys. Rev. A **93**, 032508 (2016).
[20] B. Spreng, T. Gomg, and J. N. Munday, Int. J. Mod. Phys. A **37**, 2241011 (2022).
[21] Y. S. Barash, Radiophys. Quantum Electron. **21**, 1138 (1978).
[22] S. J. van Enk, Phys. Rev. A **52**, 2569 (1995).
[23] R. B. Rodrigues, P. A. M. Neto, A. Lambrecht, and S. Reynaud, Europhys. Lett. **76**, 822 (2006).
[24] L. Chen and K. Chang, Phys. Rev. Lett. **125**, 047402 (2020).
[25] M. Antezza, I. Fialkovsky, and N. Khusnutdinov, Phys. Rev. B **102**, 195422 (2020).
[26] M. G. Silveirinha, S. A. H. Gangaraj, G. W. Hanson, and M. Antezza, Phys. Rev. A **97**, 022509 (2018).
[27] R. Requist, F. Tandetzky, and E. K. U. Gross, Phys. Rev. A **93**, 042108 (2016).
[28] M. Z. Hasan and C. L. Kane, Rev. Mod. Phys. **82**, 3045 (2010).
[29] F. Lindel, G. W. Hanson, M. Antezza, and S. Y. Buhmann, Phys. Rev. B **98**, 144101 (2018).
[30] W. Moffitt and W. Thorson, Phys. Rev. **108**, 1251 (1957).
[31] J. C. Slonczewski, Phys. Rev. **131**, 1596 (1963).
[32] L. D. Landau and E. M. Lifshitz, *Quantum Mechanics: Non-Relativistic Theory* (Pergamon Press, Oxford, 1977).
[33] M. S. Child and H. C. Longuet-Higgins, Philos. Trans. R. Soc. London A **254**, 259 (1961).
[34] P. Atkins and R. Friedman, *Molecular Quantum Mechanics*, 4th ed. (Oxford University Press, New York, 2005).
[35] E. Clementi and D. L. Raimondi, J. Chem. Phys. **38**, 2686 (1963).
[36] S. Y. Buhmann, L. Knöll, D.-G. Welsch, and H. T. Dung, Phys. Rev. A **70**, 052117 (2004).
[37] J. A. Bittencourt, *Fundamentals of Plasma Physics* (Springer, New York, 2004).
[38] J. Larson, E. Sjöqvist, and P. Öhberg, *Conical Intersections in Physics* (Springer, Cham, Switzerland, 2020).
[39] B. Göhler, V. Hamelbeck, T. Z. Markus, M. Kettner, G. F. Hanne, Z. Vager, R. Naaman, and H. Zacharias, Science **331**, 894 (2011).
[40] J. Fransson, J. Phys. Chem. Lett. **13**, 808 (2022).
[41] X. Bian, Y. Wu, H.-H. Teh, Z. Zhou, H.-T. Chen, and J. E. Subotnik, J. Chem. Phys. **154**, 110901 (2021).
[42] A. Kato, H. M. Yamamoto, and J. Kishine, Phys. Rev. B **105**, 195117 (2022).
[43] H. C. Longuet-Higgins, U. Öpik, M. H. L. Pryce, and R. A. Sack, Proc. R. Soc. London A **244**, 1 (1958).
[44] J. Fransson, Phys. Rev. B **102**, 235416 (2020).
[45] G.-F. Du, H.-H. Fu, and R. Wu, Phys. Rev. B **102**, 035431 (2020).
[46] B. P. Bloom, Y. Lu, T. Metzger, S. Yochelis, Y. Paltiel, C. Fontanesi, S. Mishra, F. Tassinari, R. Naaman, and D. H. Waldeck, Phys. Chem. Chem. Phys. **22**, 21570 (2020).
[47] W. C. Chew, *Waves and Fields in Inhomogeneous Media* (IEEE Press, New York, 1995).
[48] S. Lannebére and M. G. Silveirinha, J. Opt. **19**, 014004 (2016).
[49] K. Sakoda, *Optical Properties of Photonic Crystals* (Springer, Berlin, 2004).